

Toward Developing a Climatology of Fire Emissions in Central Asia

Authors: Park, Yun Hee, and Sokolik, Irina N.

Source: Air, Soil and Water Research, 9(1)

Published By: SAGE Publishing

URL: <https://doi.org/10.1177/ASWR.S39940>

BioOne Complete (complete.BioOne.org) is a full-text database of 200 subscribed and open-access titles in the biological, ecological, and environmental sciences published by nonprofit societies, associations, museums, institutions, and presses.

Your use of this PDF, the BioOne Complete website, and all posted and associated content indicates your acceptance of BioOne's Terms of Use, available at www.bioone.org/terms-of-use.

Usage of BioOne Complete content is strictly limited to personal, educational, and non - commercial use. Commercial inquiries or rights and permissions requests should be directed to the individual publisher as copyright holder.

BioOne sees sustainable scholarly publishing as an inherently collaborative enterprise connecting authors, nonprofit publishers, academic institutions, research libraries, and research funders in the common goal of maximizing access to critical research.

Toward Developing a Climatology of Fire Emissions in Central Asia

Yun Hee Park and Irina N. Sokolik

School of Earth and Atmospheric Sciences, Georgia Institute of Technology, Atlanta, GA, USA.

ABSTRACT: Fire emissions are a significant mechanism in the carbon cycling from the Earth's surface to the atmosphere, and fire behavior is considerably interacted with weather and climate. However, due to interannual variation of the emissions and nonlinear smoke plume dynamics, understanding the interactions between fire behavior and the atmosphere is challenging. This study aims to establish a climatology of the fire emission in Central Asia and has estimated a feedback of fire emissions to meteorological variables on a seasonal basis using the Weather Research and Forecasting model coupled with Chemistry. The months of April, May, and September have a relatively large number of pixels, where the plume height is located within the boundary layer, and the domain during these months tends to have unstable conditions at the strongest smoke, showing a lower percentage of stable conditions. From the seasonal analysis, the high fire intensity occurs in the summer as smoke travels above the boundary layer, changing temperature profile and increasing the water vapor mixing ratio.

KEYWORDS: fire emissions, wildfires, seasonality, Central Asia

CITATION: Park and Sokolik. Toward Developing a Climatology of Fire Emissions in Central Asia. *Air, Soil and Water Research* 2016;9:87–96 doi:10.4137/ASWR.S39940.

TYPE: Original Research

RECEIVED: April 13, 2016. **RESUBMITTED:** July 26, 2016. **ACCEPTED FOR PUBLICATION:** August 4, 2016.

ACADEMIC EDITOR: Carlos Alberto Martinez-Huitle, Editor in Chief

PEER REVIEW: Five peer reviewers contributed to the peer review report. Reviewers' reports totaled 1179 words, excluding any confidential comments to the academic editor.

FUNDING: This study has been supported by the NASA LCLUC Program. The authors confirm that the funder had no influence over the study design, content of the article, or selection of this journal.

COMPETING INTERESTS: Authors disclose no potential conflicts of interest.

COPYRIGHT: © the authors, publisher and licensee Libertas Academica Limited. This is an open-access article distributed under the terms of the Creative Commons CC-BY-NC 3.0 License.

CORRESPONDENCE: ypark31@gatech.edu

Paper subject to independent expert single-blind peer review. All editorial decisions made by independent academic editor. Upon submission manuscript was subject to anti-plagiarism scanning. Prior to publication all authors have given signed confirmation of agreement to article publication and compliance with all applicable ethical and legal requirements, including the accuracy of author and contributor information, disclosure of competing interests and funding sources, compliance with ethical requirements relating to human and animal study participants, and compliance with any copyright requirements of third parties. This journal is a member of the Committee on Publication Ethics (COPE).

Published by Libertas Academica. Learn more about this journal.

Introduction

Wildfires prefer warm and dry conditions, and the fires statistically occur from spring to fall (April–October) in Central Asia. Wildfires represent a significant source of aerosols and greenhouse gases, which can significantly affect the regional climate, visibility, and even global climate.^{1,2} The aerosols often react with other gases or particles in the air and influence the environment by changing the atmospheric dynamics and physics. Koren et al³ reported that the cloud coverage was reduced from 38% in clean conditions to 0% from heavy smoke during the biomass burning season over the Amazon, which implies that smoke tends to reduce the cloud coverage and precipitation.

Wildfires can release large amounts of particulate matter and other air pollutants. The increased concentrations of trace gases (eg, ozone and carbon monoxide) and aerosol particles have been observed in connection with vegetation fires in various regions of the world.⁴ Wildland fires contribute to an estimated 15% of total particulate matter and 8% of CO emissions over the southeastern U.S.⁵

Fire occurrence and intensity are related to weather and climate. Generally, a fire season is extended under warm and dry conditions, and hotter and drier conditions can cause intensifying fires.⁶ Also, fires are favorable to vegetation perishability and may influence climate through radiative energy exchange with a long-term effect.⁷ In this aspect, a feedback between climate and fires is possible because fires also modify climate.

In addition to the impact on air quality and weather, smoke aerosol can influence radiative balance and cloud microphysics. Generally, aerosols increase the cloud droplet number concentration and reduce the size of the droplets, causing less precipitation. The lifetime of clouds tends to increase in polluted areas, but this varies due to aerosol concentration and properties.⁸ Also, aerosols, such as soot, tend to absorb solar radiation more than other aerosols, which increases air temperature and can lead to cloud evaporation. In this aspect, the impact of aerosols on clouds and precipitation is important and complicated.

Satellite and in situ observations have shown an increase in fire occurrence during drought years. Severe drought reduces soil moisture, pushing the plant-available water below a critical threshold level for a prolonged period and resulting in increased fire activity. The normalized difference vegetation index (NDVI) is often used as a drought-monitoring indicator. The NDVI provides near-daily global observations of the land surface, using the visible red and near-infrared bands. Thus, the NDVI is used for the effective monitoring of droughts. Surface temperature and NDVI tend to have a negative correlation because higher temperature brings less moisture in which vegetation rarely survives. However, Karnieli et al⁹ showed that the relationship between land surface temperature and NDVI varies due to seasonal and spatial changes.



Even though the impact of fire on the climate is important, there are restrictions on our ability to understand this impact. First of all, monitoring fire emissions and plume dynamics is challenging due to insufficient in situ observations. Currently, only satellites provide the fire indicators (eg, burned area and active fire location) on a global scale with some uncertainty. Monthly fire emission estimates by various remote sensing-based techniques are varied by an order of magnitude.¹⁰ The reasons for this variability are associated with the fire estimation of burned areas caused by fuel composition, loading, vertical structure, consumption, and characterization of conditions from preceding drought and heat. Additionally, fire events vary by season, land use, and land cover types. Studies for the fire impact on regional and global climates have had a large variability of fire emissions and climatic variability, such as temperature increases, precipitation changes, and high concentrations of carbon dioxide (CO₂).^{11–13} Therefore, a better understanding of the limit of fire emissions and quantifying emission data can contribute to predicting climate and air quality with higher confidence.

Fire emissions are a significant mechanism in the carbon cycling from the Earth's surface to the atmosphere, and fire behavior is considerably interacted with weather and climate. However, due to interannual variation of the emissions and nonlinear smoke plume dynamics, understanding the interactions between fire behavior and the atmosphere is challenging. The objectives of this study are twofold: first, a method is developed to establish a climatology of fire emissions in Central Asia, correcting burned areas for fire emission inputs in modeling by using the combination of two fire products from Moderate Resolution Imaging Spectroradiometer (MODIS). Second, the feedback of fire emissions on the atmospheric stability (and other basic variables on a seasonal basis) of fire emissions in Central Asia is analyzed. To support the goals of this study, the data and methodology used are described in the "Data and methods" section, the evaluation of the burned area and analysis of fire impacts are presented in the "Results" section, and conclusions and future works are presented in the "Discussion and conclusion" section.

Data and Methods

MODIS burned area product. The MODIS Collection 5.1 Direct Broadcast Monthly Burned Area Product (MCD64A1) provides the 500 m burned area with thresholds on temporal change in a burn sensitive to the vegetation index to detect burned areas, along with the approximate day of burning.¹⁴ The MCD64A1 product incorporates cumulative active fire maps to guide the selection of burned and unburned training samples for the change detection algorithm.¹⁴ This product can be downloaded from <http://fuoco.geog.umd.edu>, giving five variables: the burn date, burn date uncertainty, quality assurance, first day of burning, and last day of the burning.

Active fires. For this study, MODIS Thermal Anomalies/Fire products (MOD14A1) has been used. The fire detection algorithm is based on the absolute detection of a fire when the fire strength is sufficient to detect and on the detection relative to its background. Numerous tests have been employed to reject typical false alarm sources such as a sun glint or an unmasked coastline. The active fires are produced every eight days at a 1-km resolution, and the data can be downloaded from <https://firms.modaps.eosdis.nasa.gov/>. The active fire product is used for adjusting burned areas, which is described in the "Adjusting fire emissions" section.

MOD13C2. The MODIS NDVI product contains atmospherically corrected bidirectional surface reflectance masked for water, clouds, and cloud shadows. Global MOD13C2 data are the cloud-free spatial composites of the gridded 16-day, 1-km MOD13A2 and are provided monthly as a Level 3 product projected on a geographic climate modeling grid. Vegetation indices for globally monitoring vegetation conditions are used in products displaying land cover and land cover changes. These data are used for investigating fire behaviors in this study.

The model description and study area. Central Asia is bounded by Russia on the north and by Iran on the south and consists of vast grassy steppes of Kazakhstan in the north and the Aral Sea drainage basin in the south. Because of more than 50% of the region covered with desert, Central Asia suffers from very dry climatic conditions and insufficient precipitation. The region as a whole experiences hot summers and cool winters, with much sunshine and very little precipitation.

To investigate the fire impacts in Central Asia, we run the Weather Research and Forecasting model coupled with Chemistry (WRF_Chem model; Version 3.6) with the following configurations. The horizontal resolution is 10 km over Central Asia (Fig. 1; longitude: 40E–100E, latitude: 30N–60N). The physics options are the Morrison 2-moment scheme for the microphysics scheme, the rapid radiative transfer model (RRTM) scheme for the longwave radiation scheme, the Dudhia scheme for the shortwave radiation scheme, and the Grell–Freitas ensemble scheme for the cumulus cloud scheme. More information on the configuration is given in Table 1. Our simulation includes fire emission inputs with calculated burned areas of pixels where fires were detected. The running period of the model is from April to September in 2008, which is the fire season in Central Asia.

Adjusting fire emissions. Randerson et al¹⁵ have shown that small fire impacts are significant in burned areas. The regional climatology analysis for the active fires on burned areas has demonstrated that significant active fires may be located outside of burned areas. It varies with season, but the ratio of FC_{in} to FC_{out} is 1:1 during the growing season (April–September) over Central Asia, which supports the Randerson's approach. Thus, based on Randerson et al,¹⁵ the two satellite

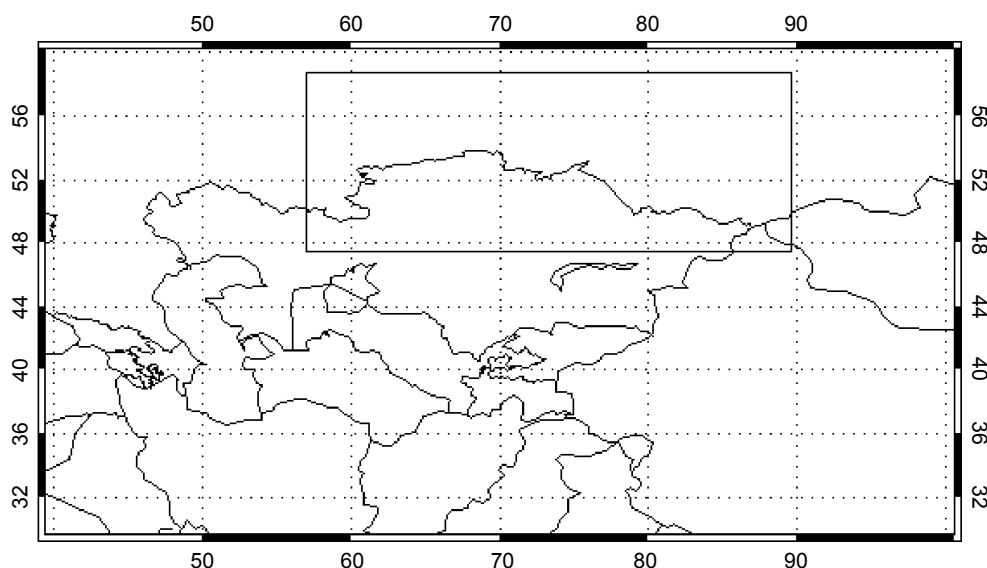


Figure 1. The WRF domain over Central Asia with 10 km × 10 km horizontal resolution. A box inside the domain is for the analysis of the feedback of smoke to basic meteorological variables (in the “Analysis of the feedback of smoke to basic meteorological variables” section).

fire products (MCD64A1 and MOD14A1) are used in our study for estimating burned areas. Randerson et al¹⁵ have suggested the following equation:

$$BA_{\text{total}} = BA_{\text{MCD64A1}} + BA_{\text{MCD64A1}} \times \frac{FC_{\text{out}}}{FC_{\text{in}}} \times \gamma, \quad (1)$$

where BA_{MCD64A1} is the burned area derived from MCD64A1, FC_{out} is the total number of active fires from MOD14A1 outside of the burned area in each model grid cell, FC_{in} is the same but within the burned area, and γ is the coefficient that modifies the burned areas with the different normalized burned ratio. If the MCD64A1 burned area is not available due to data limits, BA_{total} cannot be estimated from equation (1) by unknown value. During the study periods, the number of

pixels that were detected as burned areas from MODIS was reduced compared to a global fire inventory in the process of quality controls. To overcome the limits of data availability, if a pixel has active fires but not burned areas, the burned areas (BA_{MCD64A1}) are set to 22.8 ha as a default value.

Results

Evaluation of burned areas with the fire inventory data set. To evaluate the calculated burned areas based on Randerson et al,¹⁵ the burned areas have been compared to the values of Fire Inventory from NCAR (FINN) data. The FINN provides fire burning estimates with the daily and high resolution (1 km × 1 km) for use in regional and global models. To be consistent in the comparison, we regrid the FINN data (1 km) to the WRF_Chem domain grids (10 km). Table 2 shows the monthly values of (1) the number of pixels of burning over the domain, (2) burned area, (3) variation, and (4) the minimum and maximum values of burned area in the domain. The unit of the burned area is hectare. While burned areas (using the Randerson equation for April and May) showed still decreasing values compared to the FINN data, the statistics in other months is comparable to the FINN data.

Figure 2 shows the monthly spatial NDVI data for Central Asia in 2008. The growing season of vegetation starts in April. Most burning occurs in shrub and grassland areas from the spring to fall in which the NDVI is about 0.2–0.4, as seen in Figures 2 and 3. The correlation of the interrelationship between burned areas and NDVI was low. The relationship between burned areas and NDVI is weak because NDVI represents the vegetation growth stage. For example, moderate NDVI values (0.2–0.5) represent less dense vegetation, such as shrubs and grasslands, and high NDVI values (0.6–0.9) correspond to more dense vegetation such as

Table 1. The configuration of the WRF_Chem V3.6.

MODEL	WRF-ARW V3.6
Dynamics	Non-hydrostatic
Horizontal resolution	10 km
Domain coverage	Central Asia
Map projection	Lambert-Conformal
Horizontal grid	399 × 324
Initialization	NCEP final analysis
Radiation	RRTM (LW)/Duhia (SW)
Land surface	Noah
Cumulus	Grell-Freitas ensemble
PBL parameterization	YSU
Microphysics	Morrison



Table 2. Statistics of calculated burned areas (hectare).

[HA]	# OF PIXELS		MEAN OF BA		STDDEV OF BA		MIN BA		MAX BA	
	FINN	RANDERSON	FINN	RANDERSON	FINN	RANDERSON	FINN	RANDERSON	FINN	RANDERSON
April	12239	5395	73	40	13	71	0.75	0.83	1.00E + 02	2.22E + 03
May	6553	2501	62	40	17	96	0.75	0.83	1.00E + 02	2.46E + 03
June	1747	1740	76	69	21	122	0.75	0.83	1.00E + 02	2.14E + 03
July	2076	2333	68	71	21	179	0.75	0.83	1.00E + 02	4.34E + 03
August	4382	3616	70	64	14	139	0.75	0.83	1.00E + 02	3.74E + 03
September	2942	2440	64	30	20	101	0.75	0.83	1.00E + 02	2.68E + 03

forests. Even though the NDVI metrics and thresholds do not directly correspond to fire burning events, they provide indicators of burning preferences. Thus, from the relationship between NDVI and burned areas, we interpret that fire occurs frequently over shrubs and grasslands.

In addition, the distribution of the monthly burned areas is investigated, as shown in Figure 4. The bin size was determined by the mean values of burned areas from Table 2 and a climatology default value (22.8 ha). The blue colored sectors show where the burned areas are decreased compared

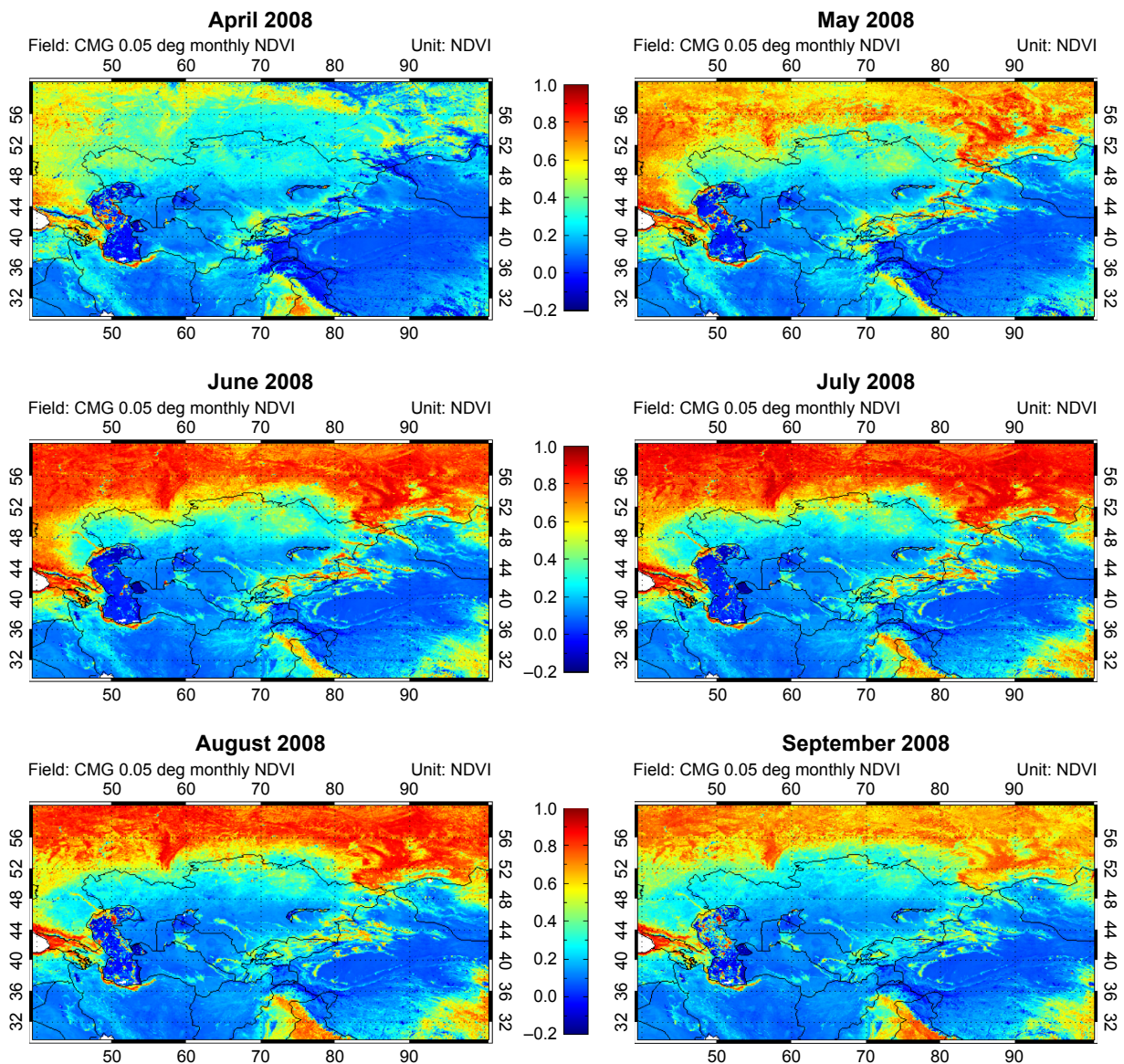


Figure 2. Spatial plots of monthly NDVI from MOD13C2.

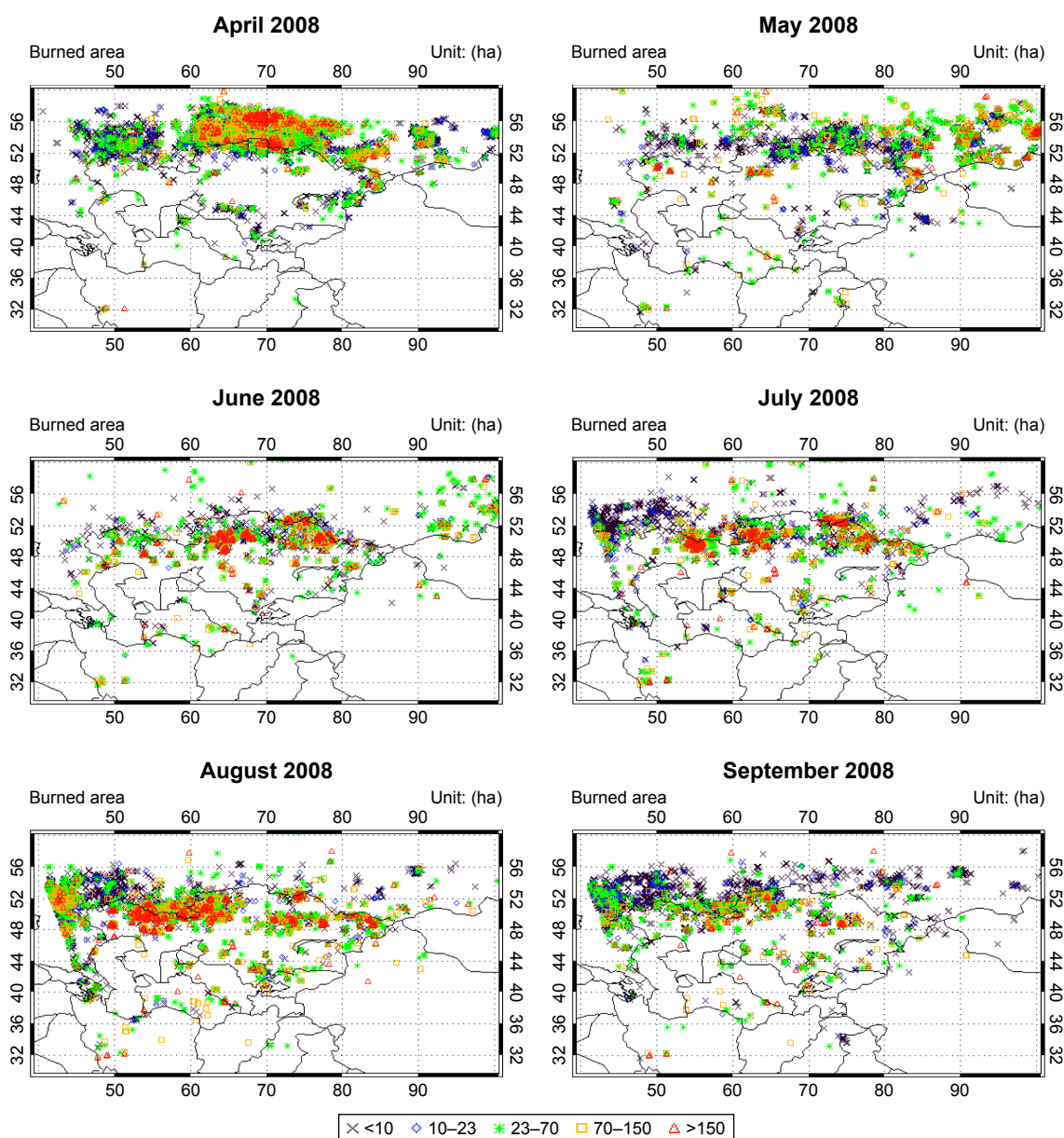


Figure 3. Calculated monthly burned area based on the Randerson's approach. Each symbol represents the range of burned areas (hectare).

to the default value, and the red colored sectors show where the burned areas are increased. According to the distribution of the burned areas, more than 50% of fire pixels show an increase in the size of burning area compared to climatological default values. The calculated burned areas are validated with the FINN data set and show a comparability of the statistics of burned areas (Table 2).

Fire occurrence and fire intensity on a seasonal basis are analyzed on the statistics of Table 2. The summer season (June and July) has a relatively small fire occurrence compared to the beginning and end of the simulation according to the number of pixels of the BA over the domain. On the other hand, the summer is a large fire intensity season by the mean of the BA. Therefore, the calculated burned areas have reasonable values for fire emissions compared to the FINN data, and the

summer season tends to show the high fire intensity with the low fire occurrence.

A feedback of the fire emission.

Analysis of the feedback of smoke to the atmospheric stability.
We examine the dependence of smoke plume height on atmospheric conditions. Smoke plume height is determined where the amount of smoke is the largest from the vertical distribution. Most smoke plumes were located above the boundary layer over the domain (90% of the domain), which indicates that smoke plumes generally travel to high altitudes. Figure 5 shows the number of pixels where smoke plumes are below the boundary layer for each month.

From the relationship between the smoke plume height and boundary layer height, the simulation of fire emissions in April, May, and September shows more plume heights

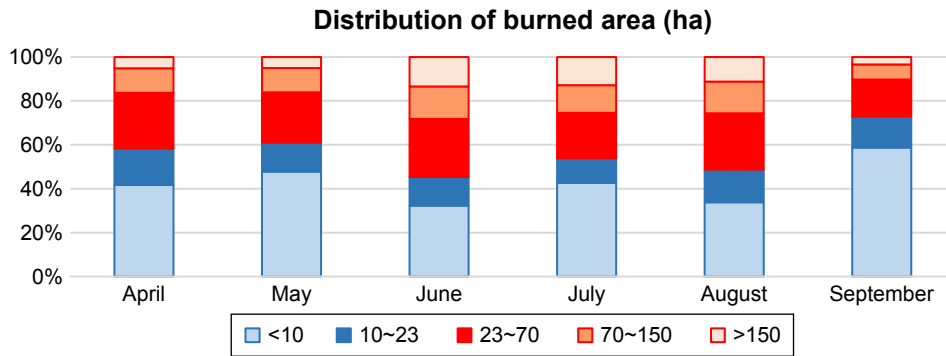


Figure 4. The distribution of burned area in Central Asia. Blue color sectors represent where the burned area is smaller than default value (22.8 ha), and red color sectors represent where the burned area is larger.

located below the boundary layer. Also, spring and fall have the highest fire occurrence and lowest fire intensity, which may increase the horizontal dispersion due to stability. On the other hand, the summer tends to have a high fire intensity and the most smoke plumes above the boundary layer, which shows a great possibility for stronger smoke travels above the boundary layer.

In addition, the dependence of smoke plume height on atmospheric stability is examined. Atmospheric stability is determined as the change in the potential temperature with change in the height of each vertical pixel.¹⁶ In each pixel, where the smoke plume is detected, we analyzed the stability using the following equation¹⁶:

$$S_j = \frac{\theta}{z},$$

where S_j is the stability, θ is the potential temperature, and z is the altitude at the model levels. From this equation, a stable condition is determined by the positive slope of the stability (S_j).

As shown in Figure 6, about 30%–50% of pixels over the domain have stable conditions at the smoke plume height.

The condition of stability is related to plume height. Summer tends to have the highest stable condition at the largest smoke plume because summer has the highest fire intensity and the number of pixels where the plume height is below the boundary layer is small. The months of April, May, and September have a lower fraction of the stable condition at the strongest smoke plume, which corresponds to a low fire intensity and a number of pixels of smoke height below the boundary layer.

Analysis of the feedback of smoke to basic meteorological variables. We examined the interrelationship of surface temperature to fire events. For this analysis, we determined the border of north Kazakhstan, where fire events occurred in all months, as a subset domain (Fig. 1). Compared to the burned area map (Fig. 3), surface temperature is decreased in the large burning area in April, shown as blue colors in Figure 7. The possible reason for this is that the decreased temperature in the large burning area is significantly related to low fire intensity and stability in which smoke tends to be trapped within the boundary layer. On the other hand, the small burning area corresponds to the increasing temperature, especially in May and September. The summer, where the fire occurrence is low and the fire intensity is high, has no significant temperature change due to smoke plumes. In this aspect,

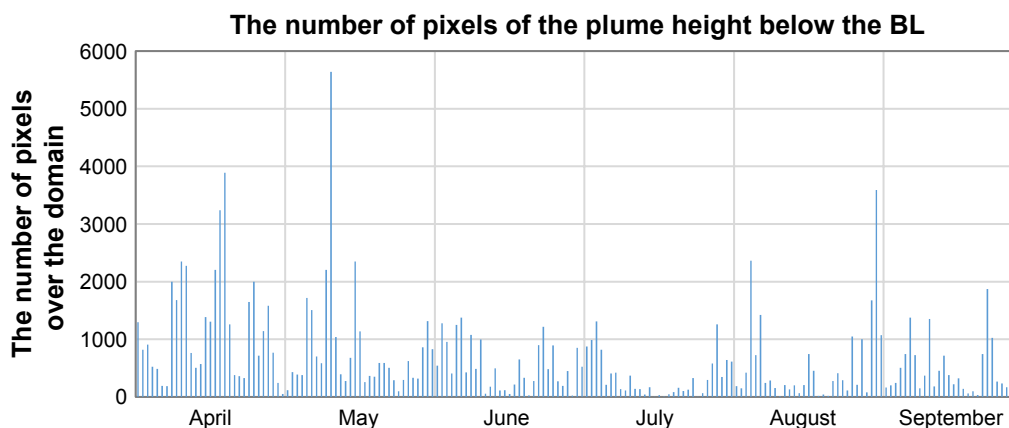


Figure 5. The number of pixels of the plume height below the boundary layer on a daily basis.

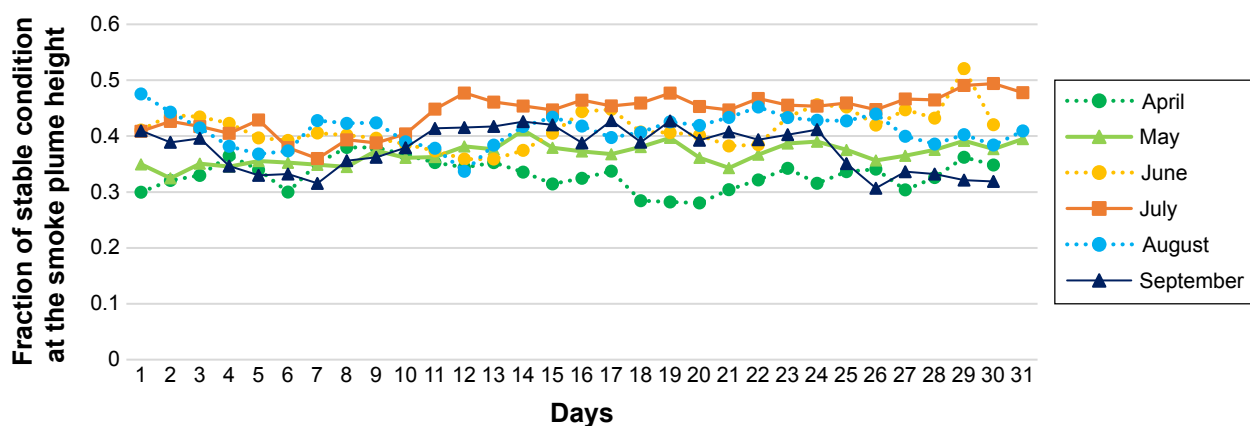


Figure 6. A fraction of stable condition at the smoke plume height on a daily basis.

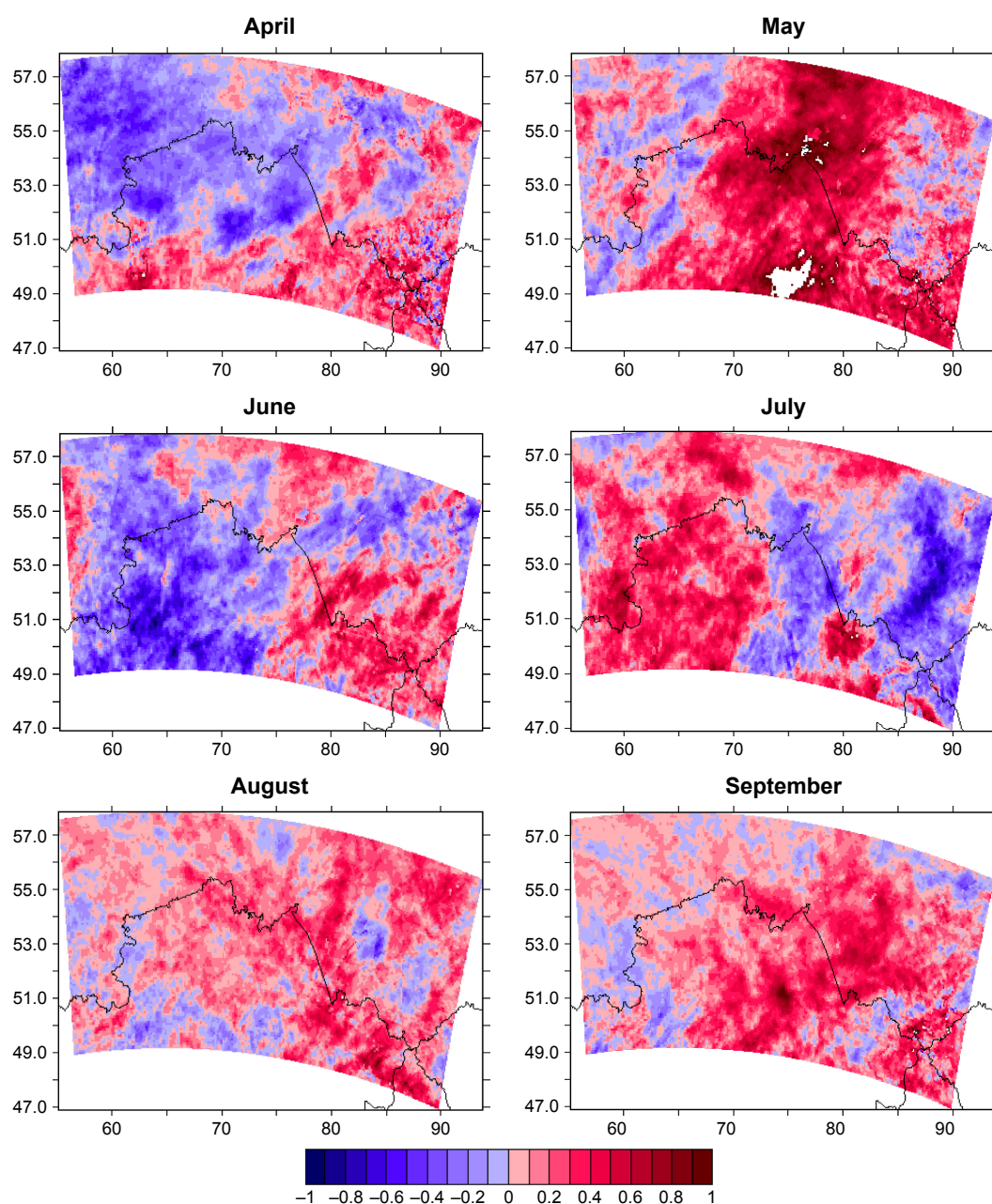


Figure 7. The difference of monthly temperature (K) at 2 m in the subdomain (WRF_Chem with fires–WRF_Chem without fires).



surface temperature is related to fire behavior and atmospheric stability as well as burning areas.

Dryness of the atmosphere during fire events was investigated for each month (Fig. 8) to understand how much atmosphere conditions are correlated with fire behaviors. The fire intensity and fire occurrence can be represented by the mean of burned areas from Table 2 and Figure 5. May is a

month of significantly increasing water vapors with the high fire occurrence. Remarkably, months of summer (eg, June and July) having the high fire intensity tend to have the increasing water vapor mixing ratio in fire locations. However, April and September, the months of the high fire occurrence, present an insignificant change of the water vapor mixing ratio. August is another month of the high fire intensity, but the

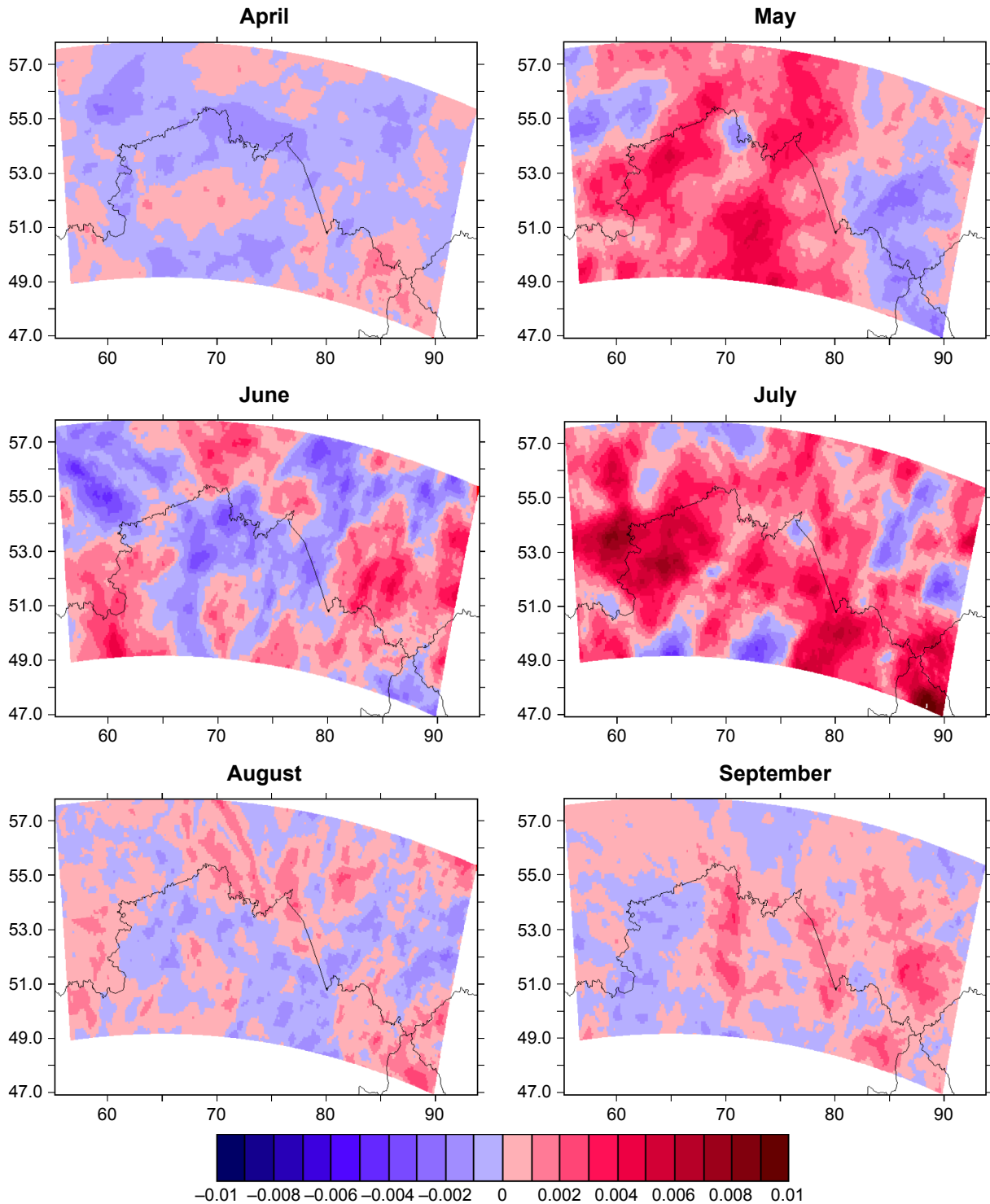


Figure 8. The difference of monthly water vapor mixing ratio (g/kg) between WRF_Chem with fire emissions and WRF_Chem without fire emissions in the subdomain.

amount of increasing water vapor in that month is relatively small. From these analyses, water vapor itself cannot explain the correlation with fire events, and temperature is an important factor in the relationship of dryness of the atmosphere and fire occurrence.

As an additional analysis, we have examined the impact of fire emissions on cloud fractions. The difference of cloud fractions between the WRF_Chem without fire emissions and

the WRF_Chem with fire emissions explains the change in the cloud spatial distribution due to fire emissions (Fig. 9). Overall, more clouds are formed in the model simulation (WRF_Chem with fires). However, the difference of monthly averaged cloud fractions does not correspond to burning areas. From the analysis of the basic atmospheric variables, intensive fire events (in summer) travel above the boundary layer and cause an increase in the atmosphere humidity.

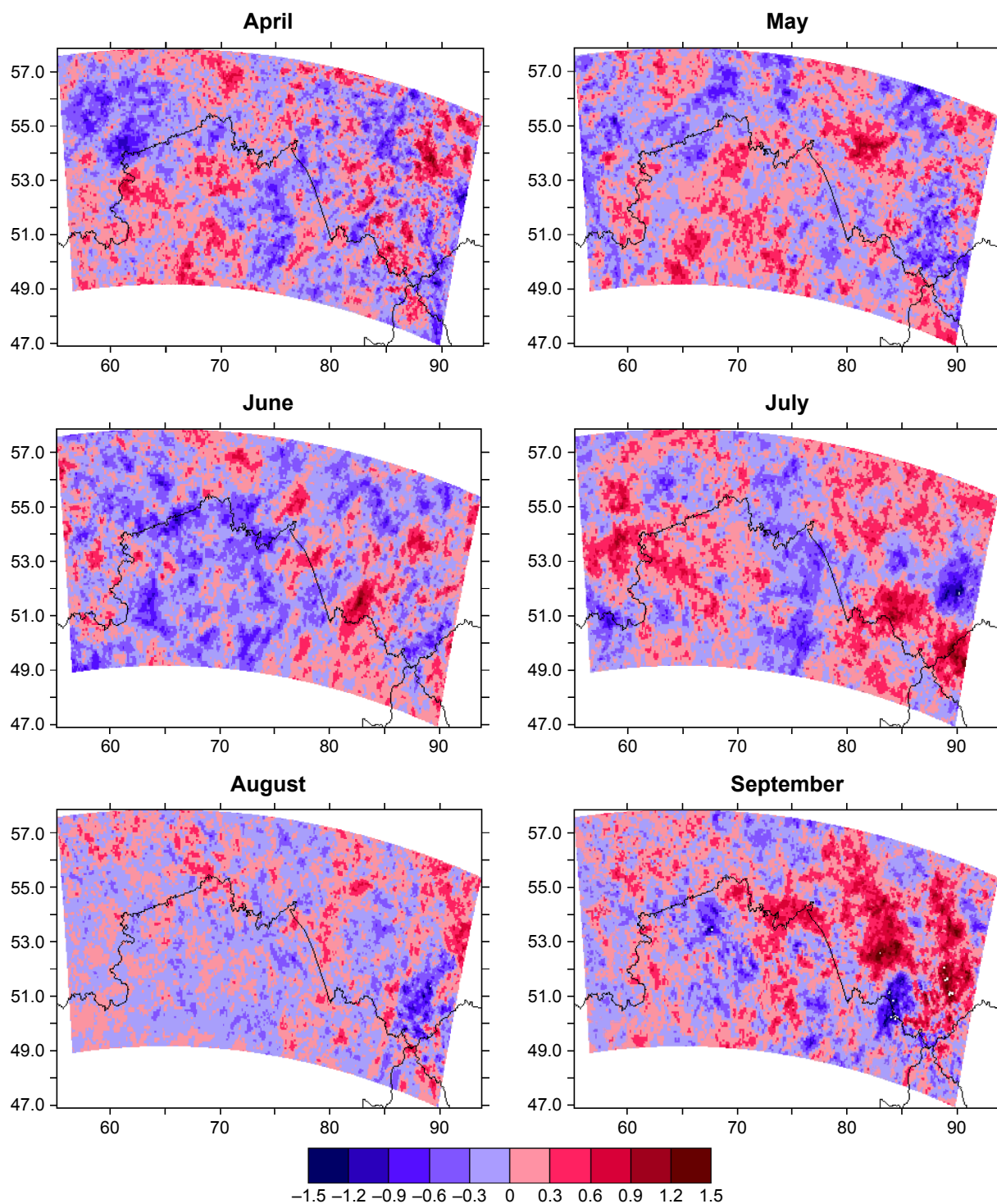


Figure 9. The difference of monthly cloud fractions between the two simulations (WRF_Chem with fires–WRF_Chem without fires).



Discussion and Conclusion

This paper deals with generating fire emissions using two satellite products and develops an approach to establish the climatology of fire events over Central Asia. The NDVI metrics provide the indicators of burning preferences even though it cannot be explained as a regression relationship with fire intensity. Calculating burned areas by equation (1), given above, still has the issue of missing data. Therefore, we decided to use the climatological value of burned area (22.8 ha), where only active fires are detected in the domain pixel. According to the distribution of burned areas, fire pixels have increased by more than 50%. Also, the summer season tends to have a high fire intensity with low fire occurrence, while spring and fall tend to have a low fire intensity with high fire occurrence.

The analysis of atmospheric stability to smoke explains that most smoke plumes are located above the planetary boundary layer. In the case of the plume being above the boundary layer, stronger smoke plumes travel to the higher altitude. These plumes are located within the boundary layer and may increase horizontal dispersion under stable conditions. From analyzing stability at the level of strongest smoke, more plume height within the boundary layer has a less stable condition.

From the analysis of basic atmospheric variables, we have investigated the importance of fire occurrence and fire intensity. Intensive fire events in the summer travel above the boundary layer and change temperature profile and water vapor mixing ratio in the atmosphere, shown as increasing instability and water vapor mixing ratio. On the other hand, the impact of high fire occurrence is not directly intercorrelated to the basic variables. Analyzing the change of horizontal and vertical fluxes can explain why surface temperature decreased in April and increased in September in the WRF_Chem, while fire emissions and change of water vapor mixing ratio were small.

Based on the seasonal analysis presented in this study, we are planning to develop a climatology of fire emissions over Central Asia. From the simulation of the WRF_Chem for a couple of decades, we will investigate the change of fire behaviors by separating flaming and smoldering combustions and the change of surface temperature and moisture profile. We are confident that, by developing the fire climatology, there will be many advances in our understanding of fire events in Central Asia.

Author Contributions

Conceived and designed the experiments: YHP, IS. Analyzed the data: YHP. Wrote the first draft of the manuscript: YHP. Contributed to the writing of the manuscript: YHP, IS. Agree with manuscript results and conclusions: YHP, IS. Jointly developed the structure and arguments for the paper: YHP. Made critical revisions and approved final version: YHP, IS. All authors reviewed and approved of the final manuscript.

REFERENCES

1. Randerson JT, Liu H, Flanner MG, et al. The impact of boreal forest fire on climate warming. *Science*. 2006;314:1130–1132.
2. Spracklen DV, Logan JA, Mickley LJ, et al. Wildfires drive interannual variability of organic carbon aerosol in the western US in summer. *Geophys Res Lett*. 2007;34:L16816.
3. Koren I, Martins JV, Remer LA, Afargan H. Smoke invigoration versus inhibition of clouds over the Amazon. *Science*. 2008;321:946–949.
4. Phuleria HC, Fine PM, Zhu Y, Sioutas C. Air quality impacts of the October 2003 Southern California wildfires. *J Geophys Res*. 2005;110:D07S20.
5. Barnard W, Sabo W. Review of 1999 NEI (Version 2. final) and recommendations for developing the 2002 VISTAS inventory for regional haze modeling (area and point sources). Prepared for VISTAS, Asheville, NC, USA. 2003.
6. Core Writing Team, Pachauri RK, Reisinger A, eds. *Climate Change: Synthesis Report. Contribution of Working Groups I, II and III to the Fourth Assessment Report of the Intergovernmental Panel on Climate Change*. Geneva, Switzerland: IPCC; 2007:104.
7. Liu H, Randerson JT. Interannual variability of surface energy exchange depends on stand age in a boreal forest fire chronosequence. *J Geophys Res*. 2008;113:G01006.
8. Xue H, Feingold G, Stevens B. Aerosol effects on clouds, precipitation, and the organization of shallow cumulus convection. *J Atmos Sci*. 2007;65:392–406.
9. Karnieli A, Agam N, Pinker RT, et al. Use of NDVI and land surface temperature for drought assessment: merits and limitations. *J Clim*. 2010;23:618–633.
10. Al-Saadi J, Soja AJ, Pierce RB, et al. Intercomparison of near-real-time biomass burning emissions estimates constrained by satellite fire data. *J Appl Remote Sens*. 2008;2(1):021504; doi:10.1117/1.2948785.
11. McKenzie D, Gedalof Z, Peterson DL, Mote P. Climatic change, wildfire, and conservation. *Conserv Biol*. 2004;18:890–902.
12. Littell JS, Oneil EE, McKenzie D, et al. Forest ecosystems, disturbance, and climatic change in Washington State. USA. *Clim Change*. 2010;102:129–158.
13. Vose JM, Peterson DL, Patel-Weynand T. Effects of climatic variability and change on forest ecosystems: a comprehensive science synthesis for the U.S. forest sector. *Gen Tech Rep*. 2012; PNW-GTR-870. Portland, OR: U.S. Department of Agriculture, Forest Service, Pacific Northwest Research Station; 265 p.
14. Giglio L, Loboda T, Roy DP, Quayle B, Justice CO. An active-fire based burned area mapping algorithm for the MODIS sensor. *Remote Sens Environ*. 2009;113:408–420.
15. Randerson JT, Chen Y, van der Werf GR, Rogers BM, Morton DC. Global burned area and biomass burning emissions from small fires. *J Geophys Res*. 2012; 117:G04012.
16. Holton. *An Introduction to Dynamic Meteorology*. Cambridge, MA: Elsevier, Academic Press; 1992.